Particuology 104 (2025) 52–67

Contents lists available at ScienceDirect

Particuology

journal homepage: www.elsevier.com/locate/partic

Simulation of an intensive lab mixer for dry mixing of Li-ion cathode materials via the discrete element method

Clemens Lischka *, Hermann Nirschl

Institute for Mechanical Process Engineering and Mechanics (MVM), Karlsruhe Institute of Technology, Straße am Forum 8, Karlsruhe, 76131, Germany

ARTICLE INFO

Article history:
Received 24 July 2024
Received in revised form
15 May 2025
Accepted 3 June 2025
Available online 20 June 2025

Keywords:
Li-ion battery production
NMC-622
Carbon black
Dry mixing
Discrete element method
Simulation
Intensive mixer

1. Introduction and motivation

Dry mixing is an important process step in the production of Li-ion battery electrodes. It is not only the first process step, but also the one with significant influence on the performance of the manufactured electrodes. Numerous authors show that the quality of manufactured electrodes correlate with the degree of comminution of the conductive additive carbon black (Bockholt et al., 2013; Mayer et al., 2022; Wenzel et al., 2014). With the trend towards dry processing, where a second, energy-intensive mixing step with solvent is to be saved, the dry mixing as the only remaining mixing step will play the sole role of adjusting two important property-determining parameters in the electrode materials, the homogeneity and the degree of comminution of the conductive additive. In the literature, different types of mixers are used to perform dry mixing. From loose homogenization in tumble mixers (Bockholt et al., 2013) to energy-intensive mixing in Nobilta or Eirich high-intensive mixers; extruders and ball mills are also discussed (Asylbekov et al., 2023; Frankenberg et al., 2024; Guan et al., 2024; Mayer et al., 2020). However, the two most important parameters that describe the mixing process, the mixing time and the mixing intensity, usually depend on the mixer type and are found for a material system with increased experimental effort through trial and error processes. For a type of mixer that is widely used in research and industrial applications, the Eirich intensive mixer, a systematic investigation of the various process parameters and operating modes will be carried out here with regard to their potential influence on the comminution and homogenization of the conductive additive.

The Erich intensive mixer is used in literature for different types of applications. For example, the use for granulation, agglomeration or coating tasks is mentioned. Eirich RV02, EL1.0, RV01 mixers are used for this purpose, in which mixed materials such as lactose, calcium carbonate, acrylonitrile butadiene styrene (ABS) and others are processed with a generally aqueous liquid and with the addition of binders. The mixer then fulfills the task of homogenizing and agglomerating the starting materials into larger heteroagglomerates (Al hassn et al., 2018; Ax et al., 2008; Daumann et al., 2010; Muthancheri et al., 2021). The use of Eirich mixers for crushing particles in the recycling of cement (Moreno-Juez et al., 2021) and the treatment of sandy soils (Tokoro et al., 2012) was also examined. Bockholt et al. (2013) and Mayer et al. (2022) describe the use of the Eirich RV02Vac in the production of Li-ion cathodes. However, their usage always followed the two-stage mixing process, in which the Eirich mixer was used for dry mixing of cathode material and then further processing into a coatable slurry took place with addition of the solvent N-Methyl-2-pyrrolidone (NMP). Both authors emphasize that the selected process parameters for mixing time and mixing intensity in the Eirich mixer have a significant influence on the resulting cell performance. In particular, maximum intensity and mixing time are not regarded as the optimal settings. The same was also found in a previous work (Lischka et al., 2024), in which short but intensive mixing led to optimal electrical conductivity of the cathode powder materials, which was viewed as an indicator of the expected capacity of finished cathodes. Since finding optimal operating parameters on an Eirich intensive mixer requires time and materials, this work aims to use a simulation method that enables a deeper mechanistic understanding of the mixing process to be achieved through process modeling. The discrete element method (DEM) is often used in the literature to describe the flow and stress behavior of powdery and cohesive bulk materials. Although the

* Corresponding author.
E-mail address: clemens.lischka2@kit.edu (C. Lischka).

https://doi.org/10.1016/j.partic.2025.06.002

method is widely used in the literature, there are only a few works to date on simulating the Eirich mixer. The methodology is described for the first time by Tokoro et al. (2009) for modeling an R02 Eirich mixer. The authors used the DEM simulation results of energy dissipation for a population balance model to describe the crushing behavior of bauxite particles. Gong et al. (2019) and Zuo et al. (2021, 2023) use the DEM method to investigate the mixing behavior in an Eirich EL10 of iron particles with the addition of liquid for different density ratios of the used materials. Moreno-Juez et al. (2021) use DEM simulation to correlate the energy dissipation during the mixing process with the rate of mass loss due to crushing of cement. For a different type of mixer, the Nobilta annular gap intensive mixer, two papers by Asylbekov et al. (2023) and Frankenberg et al. (2024) can be found in the literature regarding the use of the DEM methodology in the production of batteries. The numerical method of Computational Fluid Dynamics (CFD) for simulating the Eirich mixer is also described by Niedziela et al. (2015) and Al Alaween et al., 2017. However, this approach is usually almost exclusively used to describe continuous Newtonian and non-Newtonian fluids and not cohesive powders as in case of this work.

2. Materials and methods

The modeling of the dry mixing process is carried out for two Eirich laboratory mixers, the EL1.0 and EL0.1, with 1l and 0.1l maximum filling volume. Fig. 1 shows the Eirich EL1.0 mixer with its internals. It consists of the fast rotating mixing tool, a rotating mixing container and a fixed wall scraper with the function to feed material into the mixing tool zone.

Building on previous experimental work (Lischka et al., 2024), the mixing process will be modeled and analyzed in this work. The Eirich mixer has a variable speed mixing tool that is available in different form factors from the manufacturer. The so-called Z-Wirbler (see Fig. 16) with downward-pointing pins was used for the experimental work. A wall scraper is also installed, which, in combination with the eccentrically installed mixing tool, ensures an asymmetrical flow in the vessel. Like the internals, the vessel is made of stainless steel and can rotate around its own axis at two different speeds of 85 rpm or 170 rpm. In addition, the inclination of the entire mixing vessel including its internals can be adjusted around a horizontal axis. It is also possible to operate the mixer in co-current or counter-current regarding the tool and vessel rotation. The mixing tool can be operated in a circumferential speed range between 5 m/s and 30 m/s. By introducing a dimensionless number, it has already been shown that the comminution process

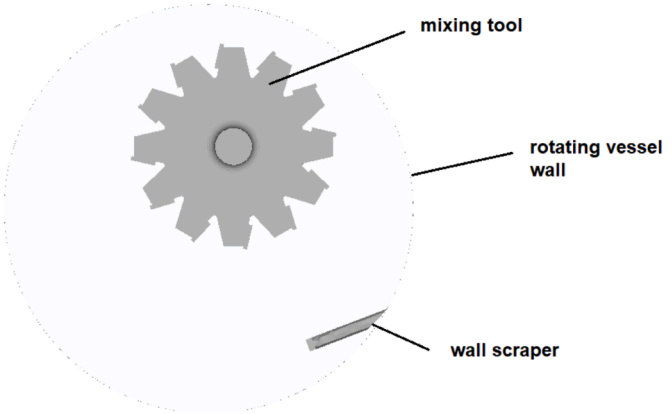

Fig. 1. Scetch of the Eirich EL1.0 mixer with internals.

of the conductive additive, described by change in the bulk density, is size independent and therefore scalable in both mixer types EL1.0 and EL0.1. Mixtures of nickel-manganese-cobalt oxide (BASF NMC622) cathode active material and carbon black Super C65 (two % mass fraction) were assumed in this work as the basis for the simulation model in accordance with previous experimental work (Lischka et al., 2024). Simulations of the EL1.0 and EL0.1 mixer were used as a validation basis with regard to the power draw of the mixing tool. A more detailed analysis was then carried out exclusively for the EL1.0 mixer. The simulation parameter variation was carried out with regard to tool speed, vessel speed, vessel inclination, vessel filling level, design of the mixing tool, direction of tool rotation and the size of the mixing tool.

2.1. DEM simulation model setup and calibration

The modeling of the flow behavior of the cathode mixture examined is based on the discrete element method (DEM), in which the description of the movement of individual particles results from a balance of all forces acting on them. The interaction of the particles with each other or with the mixer geometry takes place via contact models that take into account the particle properties, in particular the frictional forces of the material pairings. Static and rolling friction parameters as well as cohesion forces are inaccessible to direct and independent measurement, which is why comparison with so-called calibration experiments is long established. The particle sizes of the investigated system of active material NMC and carbon black in the order of μm to nm also make it necessary to use the so-called coarse graining approach in which the simulation particles are made larger by a constant Coarse Grain Factor (CGF) than reality. Since the DEM model calibrated in this way delivers acceptable results in describing the flow behavior, the particle-mixer interaction can be simulated on a technically relevant scale and not just on the microscale level. Fig. 2(a) shows schematically the DEM modeling approach, and Fig. 2(b) shows the calibration experiments used. The individual simulated particles contain a mixture of NMC622 and carbon black material in this work. The influence of the comminution of the carbon black agglomerate structures is reflected by a change in particle size, an increase in the bulk density and a reduction in the coefficient of friction, which was also found experimentally in our previous work. A detailed description of the DEM methodology and also the calibration simulations used for the coarse grain approach is described in ref. (Lischka & Nirschl, 2023). The material parameters used for the DEM simulations in this work are shown in Table 1.

2.2. Scaling of cohesion forces

For modeling the interaction of particles not only the friction parameters are of importance, for highly cohesive systems with small particle diameters the surface interactions such as the Van-der-Waals forces are of considerable influence. These forces impact the overall flow of the particles and act on the mixing behaviour as well as the power consumption of the mixing tool. We calibrated the surface energies for 2 mm DEM particles to our experiments, however for a study of particle size on the simulation results the question arises of how the surface energies should be changed to acknowledge the fact that smaller particles have a higher surface to volume ratio than larger once. To answer this question we adopted the work by Behjani et al. (2017) who introduced a cohesion number that allows to scale particles in regard to an original system. The cohesion number sets the work of cohesion in relation to the gravitational potential energy, which

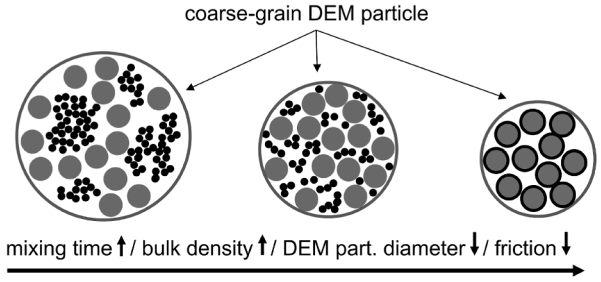

(a) Coarse-Grain DEM model: increasing mixing time correlates to higher bulk density, lower filling height in the mixing vessel (captured by smaller particle diameter) and lower friction coefficients

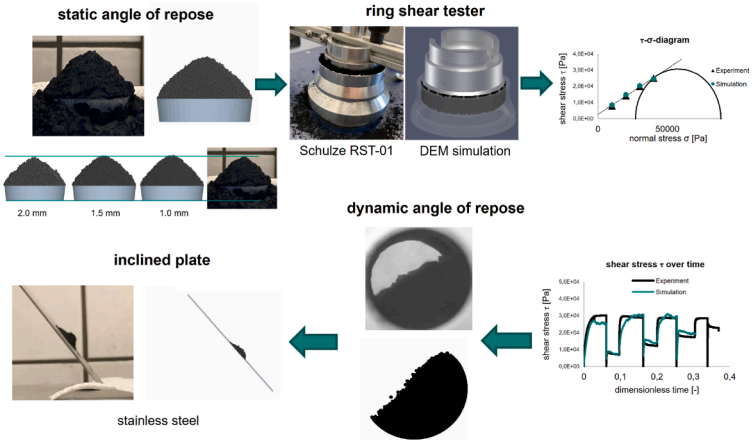

(b) Different experiments used to calibrate DEM material parameters

Fig. 2. DEM simulation approach for modeling NMC-622 and carbon black Super C65 mixtures.

Table 1
DEM simulation parameters used for different stages of comminution in accordance with mixing time and mixing tool speed.

Mixing time t_{mix}	Particle diameter	Density ρ_{bulk}	Stat. friction p-p $\mu_{s,pp}$	Dyn. friction p-p $\mu_{d,pp}$	Stat. friction p-w $\mu_{s,pw}$	Dyn. friction p-w $\mu_{d,pw}$	Cohesion energy p-p γ_{pp}	Cohesion energy p-w γ_{pw}
0 min (30 - 20 m/s)	2.0 mm	1200 kg/m^3	1.0	0.1	1.2	0.1	0.3 J/m^2	0.05 J/m^2
30 min (30 m/s)	1.757 mm	1817 kg/m^3	0.504	0.0249	0.558	0.024	0.238 J/m^2	0.039 J/m^2
30 min (25 m/s)	1.768 mm	1781 kg/m^3	0.504	0.025	0.559	0.025	0.239 J/m^2	0.0395 J/m^2
30 min (20 m/s)	1.772 mm	1768 kg/m^3	0.505	0.0252	0.56	0.026	0.24 J/m^2	0.04 J/m^2
90 min (30 - 20 m/s)	1.723 mm	1938 kg/m^3	0.5	0.025	0.55	0.025	0.236 J/m^2	0.0393 J/m^2

should always be maintained as constant for a scaled version of any original system.

$$Cohesion\ number = \frac{work\ of\ cohesion}{gravitational\ potential\ energy} \tag{1}$$

When using the Johnson-Kendell-Roberts (JKR) contact model the work of cohesion is given by the expression $7.09\left(\gamma^5 R^{*4} E^{*2}\right)^{\frac{1}{3}}$. In this γ is the surface energy between the interacting materials in J/m^2, R^* the equivalent radius of the species involved in the contact, calculated by $R^* = \left(\frac{1}{R_1} + \frac{1}{R_2}\right)^{-1}$, E^* the equivalent Young's modulus, calculated with $E^* = \left(1\frac{-\nu_1^2}{E_1} + 1\frac{-\nu_2^2}{E_2}\right)^{-1}$ (E being the Young's Modulus and ν the Poisson ratio of respective particle) and g the gravitational constant. The gravitational potential energy of a particle can be expressed as mgR^* or equivalently by $\rho R^{*3} g R^*$. With that we arrive at the final expression for the cohesion number of:

$$Coh = \frac{1}{\rho g}\left(\frac{\gamma^5}{E^{*2} R^{*8}}\right)^{\frac{1}{3}} \tag{2}$$

Although the cohesion number would theoretically allow to calculate the cohesion work of the real world particle system, we use it here to calculate the necessary surface energy γ when scaling our calibrated DEM simulation model for a study of the Coarse Grain Factor. One difficulty of using it for the real particle system lies primarily in the fact that the surface energy between NMC and NMC particles is unknown and difficult to measure. Since we calibrated the coarse grained DEM model parameters to experiments, we can nevertheless use Eq. (2) to find the necessary surface energy for particle diameters of 1.5 mm and 1 mm to study the effect of the Coarse Grain Factor. Table 1 gives these values. It should be noted that for scaling the particle wall surface energies, the diameter of the wall can not be set to a meaningful value since the contact area would be very large compared to that of the particle in contact. This would result in unrealistically high surface energies. Instead we use the same scaling factors of the particle-particle contacts and apply them to the wall surface energy of the original system at 2 mm. The resulting values are given as γ_{pw} in Table 1.

The shear modulus of the geometry material was set to 1e11 Pa. A solids density for stainless steel of 7650 kg/m^3 and a Poisson ratio of 0.25 was used in all simulations. For the cathode materials different densities, particle diameters, static and dynamic friction coefficients as well as cohesion energies were used in accordance to the state of mixing degree that was simulated (see Table 1). However a constant shear modulus of 1e8 Pa and a constant Poison ratio of 0.25 was used in all simulation cases to minimize the computational cost associated with higher shear moduli. Since the coefficient of restitution is very difficult to obtain experimentally for pure substances and basically impossible to measure for a mixture of two different species in a bulk at the same time, it was assumed to be constant at a value of 0.5 for all simulation cases. The simulation time step size was fixed at a value of 20 % of the Rayleigh time step for all simulations to guarantee a good compromise between accuracy and simulation speed. All simulations were performed until a quasi-static flow behaviour was established in the mixer which was usually achieved after a simulation time of at least 30 s. The DEM software EDEM 2022.3 was used and the simulations were performed on a Nvidia RTX-2080Ti GPU.

2.3. Collision energy transfer

By simulating the comminution process in the Eirich mixer the DEM method calculates the energy transfer by collision of particles with the rotating mixing tool. This results in the collision frequency, which is the number of completed contacts of particles with the mixing tool during a specific time interval. On the other hand the relative collision velocity v_{rel} between every particle and the mixer geometry can be accessed for each collision event. With the relative collision velocity in normal direction the collision energy transferred between the mixing tool E_{tool} and a particle during collision can be calculated as:

$$E_{coll} = \frac{m_{part} m_{mt}}{2(m_{part} + m_{mt})} v_{rel}^2 \left(1 - k^2\right) \tag{3}$$

Where m_{mt} and m_{part} stand for the mass of the mixing tool and the colliding particle respectively. The factor k represents the restitution coefficient with a constant value of 0.5. Since the mass of the mixing tool geometry is well above that of a particle during collision, we can state that $m_{part} + m_{mt} \approx m_{mt}$. Eq. (3) can then be simplified to:

$$E_{coll} = \frac{m_{part}}{2} v_{rel}^2 \left(1 - k^2\right) \tag{4}$$

The collision energy is calculated for each individual particle and summed to give the total collision energy for a time interval of 1 s. The dissipated energy in normal direction is regarded as the upper limit for the energy that can be converted to break the carbon black aggregate and agglomerate structures (Burmeister et al., 2018; Rumpf, 1959). Usually, the carbon black comminution in context of LIB production is described as a function of shear rate in the process for wet slurries. In light of dry mixing this will be discussed further in the result section.

3. Experimental results

Analyzing the mixing results of the EL1.0 and EL0.1 for different mixing tool speeds we found that the change in bulk density is strongly correlated to the measured specific energy input of the mixing tool during mixing (see Fig. 3(a)), which is expected since change in bulk density is attributed to the comminution of the carbon black. The energy input is measured via torque directly in the Eirich EL mixers. The bulk density was measured via volume and mass measurements in a small sample cylinder (Lischka et al., 2024).

The course of data points in Fig. 3(a) can be described by a function introduced by Schilde. In his work, the energy input in wet dispersion processes is used to model the change in particle size during shear mixing in dissolvers and roller-mills (Schilde et al., 2010). We adapt the model here to relate the change in bulk density ρ_{bulk} in the intensive dry mixing process of Eirich mixers as:

$$\rho_{bulk}(t) = \rho_{bulk,t=0} + \left(\rho_{bulk,t=\infty} - \rho_{bulk,t=0}\right) \frac{e_{tot}(t)}{e_{tot}(t) + K_t} \tag{5}$$

In Eq. (5), the change in bulk density $\rho_{bulk}(t)$ can be described as a function of change in mass specific energy input $e_{tot}(t)$ during mixing with the bulk density at start $\rho_{bulk,t=0}$ and the bulk density for infinite energy input $\rho_{bulk,t=\infty}$, which is defined as the maximum achievable bulk density. The parameter K_t is a process and material specific coefficient, giving the energy needed to achieve 50 % of the final bulk density $\rho_{bulk,t=\infty}$. Data regression yields a very good agreement with the model, especially in the lower and upper limit of measured values. The maximum achievable bulk density was found to be 1,83 g/mL which is 3 % higher then the highest measured value in experiments, indicating carbon black comminution can be regarded as virtually complete.

In order to verify the bulk density measurement method for determining carbon black comminution, the equivalent particle diameter of carbon black was determined using Lumisizer (LUM GmbH) sedimentation measurements. For this purpose, suspensions of mixtures were diluted with water, which were then centrifuged in the Lumisizer. Due to the high densities, rapid settling of the active material is achieved. The lighter carbon black particles sediment more slowly. An equivalent diameter of the carbon black can be calculated from the turbidity in the suspension using the Stokes approach. The course of the mean particle diameter of carbon black determined in this way is shown in Fig. 3 (b). It can be seen that the mean equivalent particle diameter decreases with increasing bulk density. For the investigated bulk density range between 1000 kg/m^3 and 1800 kg/m^3, the mean carbon black diameters are between 2.5 µm and 1 µm. This confirms that the bulk density is a direct measure of the degree of comminution of the carbon black in the mixtures. However, the absolute values determined are of limited reliability due to the measurement methodology used. For example, it cannot be ruled out that suspension of carbon black is complete, in particular of larger agglomerates, and additional energy input does not take place during the preparation of the suspensions. Furthermore, carbon black deposited on the surface of the NMC can be centrifuged with the active material and thus separated prematurely, so that the measurement is skewed. In addition, measuring the particle size distribution using the Lumisizer is generally more time-consuming than measuring the bulk density of dry mixtures. The values shown are therefore primarily used as confirmation of the correlation between energy input and bulk density of carbon black comminution.

In the literature of comminution power laws similar to the one we found in our experiments (Fig. 3(a)) have widely been adopted to describe the energy need to break up particles. Different authors presented data mainly from the mineral industry such as Rittinger, Bond and Kick. The authors find different sloping coefficients to their power law functions which is attributed to the different size ranges each authors studied. The main difference form our approach is that in the literature usually energy input is plotted against particle size and not the bulk density as in our case. In Fig. 4, the additional energy needed to process carbon black is plotted against the mixing time for three different mixing tool speeds in the EL1.0 mixer. We calculated this energy by measuring the energy input E_{total} for the total system containing the NMC/carbon-black mixture and subtracting the mixing tool energy required without any material in the mixer E_{empty} and the energy required for mixing 700 g of pure NMC-622 E_{NMC} without addition of any carbon black at the respective mixing tool speed.

$$E_{CB} = E_{total} - E_{idle} - E_{NMC} \tag{6}$$

As can be seen from Fig. 4, the specific energy used for overcoming the additional frictional forces from the addition of carbon black is the highest for the highest mixing tool speed w_{tool} of 30 m/s, followed by 25 m/s and 20 m/s which can be explained by the higher kinetic energy transferred to the material through the mixing tool. With increasing mixing time the values drop to a nearly zero at the maximum mixing time of 90 min, which indicates that comminution has decreased the frictional forces at this stage. Further mixing may likely not accomplish any more comminution of carbon black, also evident from bulk density

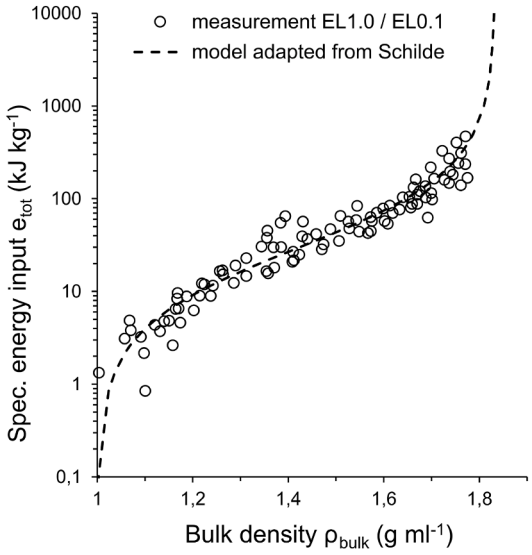

(a) Experimental results for the total specific energy input in kJ/kg over bulk density in EL1.0 & EL0.1

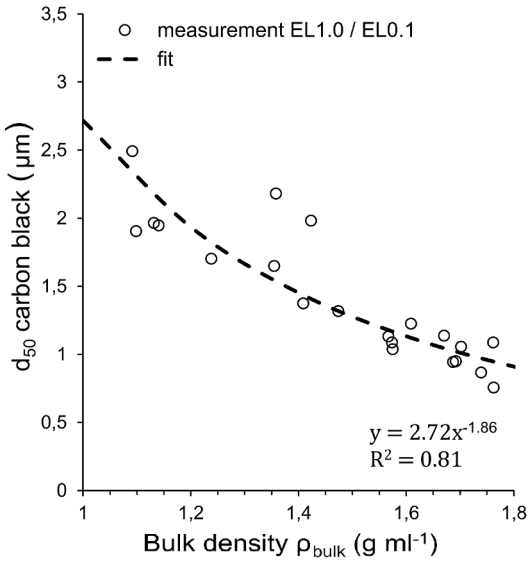

(b) Carbon black equivalent diameter d_{50} over bulk density

Fig. 3. Experimental results for the specific energy input and equivalent carbon black particle diameter during mixing.

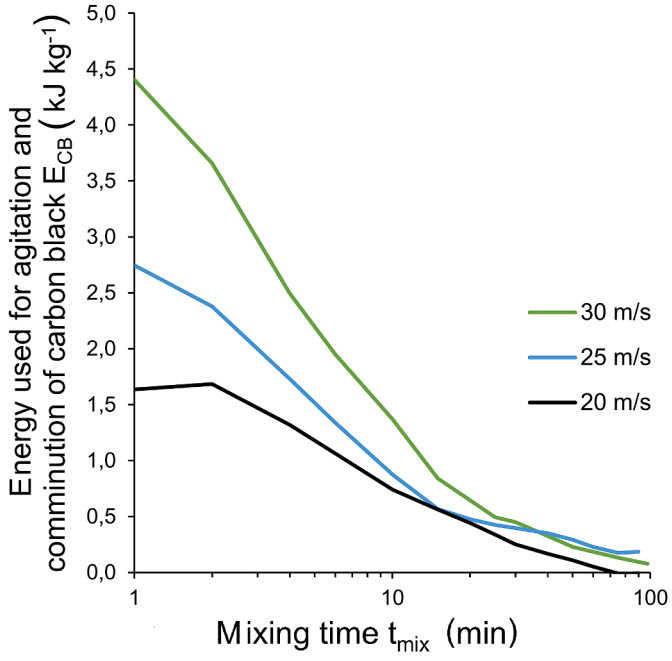

Fig. 4. Specific comminution energy during dry mixing including frictional energy for different mixing tool speeds in EL1.0 mixer.

measurement, as the energy input is not high enough to facilitate much additional breakage of carbon black structures. The overall decrease in values for E_{CB} can be explained with increased energy needed to break smaller particles, so that the highest comminution energy usage is in the beginning of dry mixing where coarse particles break more easily than at a later stage, where smaller particles have a higher energy demand to break. There are also higher frictional losses at the start of process which was confirmed by previous ring shear cell measurements (Lischka et al., 2024). We can define the relative energy utilization for agitation and comminution η_{cb} as the ratio between the specific energy usage for mixing with carbon black E_{CB} and the net energy input E_{net} at a given mixing tool speed to analyse the efficiency at which the energy is used to agitate and break the carbon black particles. The values are given in Table 2 and show that the highest efficiency of around 58 % is achieved in the beginning of mixing for the highest mixing tool speed of 30 m/s. From this analysis it is recommended to perform the dry mixing at the highest mixing tool velocity of the EL1.0 for the best utilization of energy input to perform the comminution task.

4. Simulative results

4.1. Mixing tool power consumption

We use the time averaged mixing tool power for different mixing tool speeds as a parameter to validate our DEM simulation model. As can be seen from Fig. 5(a), generally speaking the power requirement in watts increases with increasing mixing tool speed in a power law function. The mixing tool power P_{tool} is directly measured in the Eirich mixers and is calculated as the net power input after subtracting the power drawn when mixing with zero mass. The lines in Fig. 5 give the simulation results for the EL1.0 (dashed lines) and the EL0.1 (solid lines) at mixing tool speeds of 5 m/s, 10 m/s, 15 m/s, 20 m/s, 25 m/s and 30 m/s. Since material for the experiments was limited not all of these tool speeds were tested in the experiments. However it can be seen from the data that the trend is well captured by the DEM simulation model. The time averaged mixing tool power in the simulations was calculated from the formula $P_{tool} = 2\pi nM$, where n is the amount of revolutions of the mixing tool per second and the M the total torque of

Table 2
Values for agitation and comminution efficiency η_{cb} of carbon black during mixing in EL1.0

w_{tool}	η_{cb} (t_{mix} < 1 min)	η_{cb} (t_{mix} = 90 min)
30 m/s	0.58	0.02
25 m/s	0.48	0.05
20 m/s	0.42	0.00

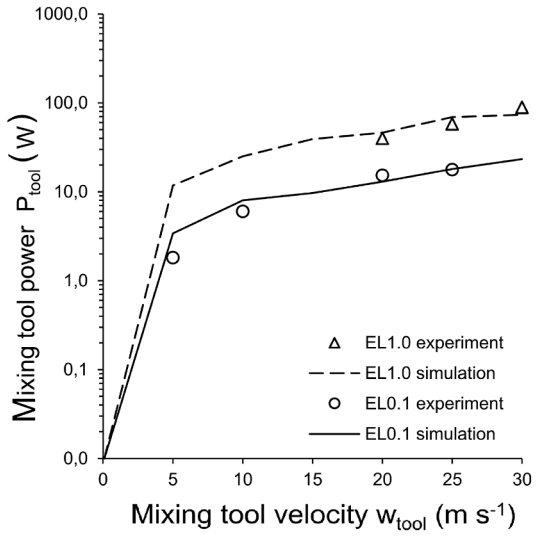

(a) Average mixing tool power P_{tool} in experiment and simulation

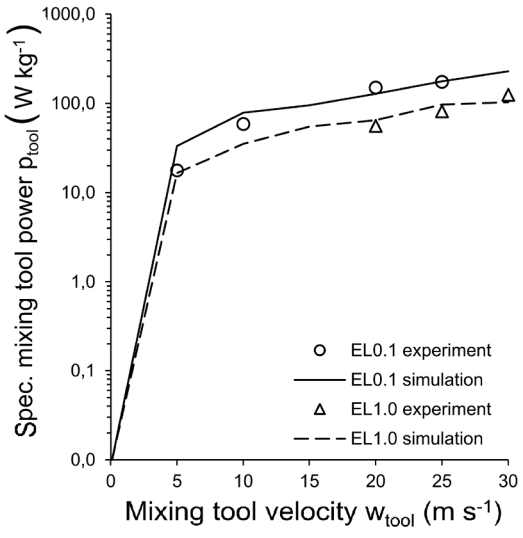

(b) Average specific mixing tool power p_{tool} in experiment and simulation.

Fig. 5. Comparison between experiments and simulations for the power draw of the mixing tool in EL1.0 and EL0.1 at the start of the mixing process t_{mix} = 0.167 min.

the mixing tool in Nm. When we calculate the mass specific mixing tool power p_{tool} (Fig. 5(b)) the EL0.1 shows a little higher values compared to the EL1.0. We attribute this difference to the higher filling ratio at the start of mixing in the EL0.1.

4.2. Comminution simulation

When looking at the tool performance for a constant circumferential speed, it is noticeable that this decreases continuously over the mixing time of up to a maximum of 90 min. As already shown earlier (Fig. 4), as the degree of comminution of the conductive additive increases with higher mixing time, the required power of the mixing tool becomes smaller, which results from a reduced friction within the material mixture. In order to simulate this time dependency, the material parameters were adjusted for three different speeds of 20, 25 and 30 m/s so that the reduced power requirement of the mixing tool could be shown for two additional mixing times at 30 min and the final state at 90 min. Since a reduced bulk density is accompanied by a reduced filling level in the mixer, particle diameter and bulk density were adjusted so that they fit the measured bulk density and the corresponding fill level in the mixer. The simulation parameters used for this can be found in Table 1. Fig. 6 shows the experimental progress of the power requirement of the mixing tool in the Eirich EL1.0 mixer, as well as the associated simulation-determined power draw. It turns out that the adapted simulation model is able to represent the reduced power requirement of the mixing tool in good agreement.

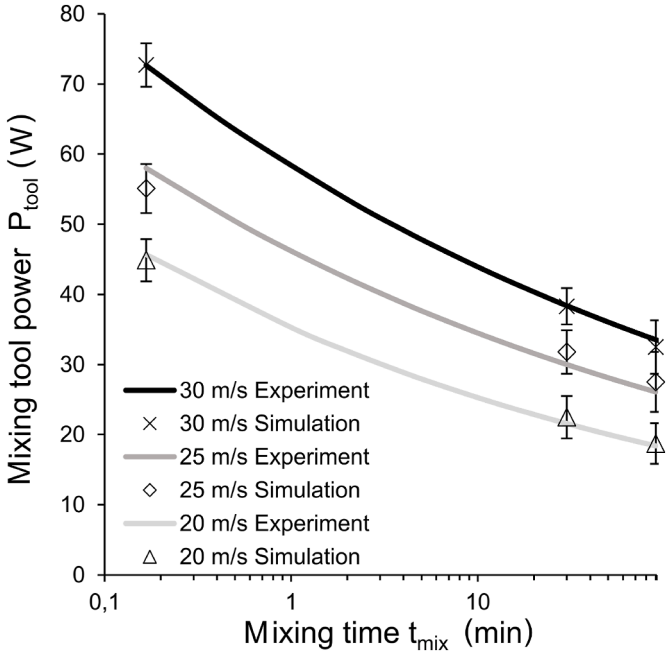

Fig. 6. Mixing tool power draw in EL1.0 mixer during comminution of carbon black, solid lines are derived from the cumulative energy input, symbols are simulation results at 0.167 min, 30 min and 90 min for three different mixing tool speeds.

4.3. Mixing efficiency

To assess the mixing quality and, in particular, the mixing time, the value of the relative standard deviation (RSD) is calculated using formula (7).

$$RSD(t) = \frac{\sqrt{\frac{1}{n_s}\sum_{n=1}^{n_s}(x_i(t) - x_t)^2}}{x_t} \tag{7}$$

This contains the number of samples n_s, the current sample concentration $x_i(t)$ and the target concentration x_t, which was set to $x_t = 0.5$ for all simulations. The minimum possible mixing quality for a stochastic random mixture RSD_s depends on the number of elements in a sample s and can be calculated using the formula $RSD_s = x_t\ (1\ -\ x_t\ )\frac{1}{s}$. With a required particle count of at least 400 particles in each tested sample, this value is 0.000625. The number of samples was set to at least 100. Fig. 7 shows progress of the mixing quality value *RSD* for different mixing tool speeds and vessel speeds plotted against the dimensionless mixing time. The mixing process starts in a completely segregated state of all particles corresponding to a *RSD* value of 1. The maximum simulation time was 30 s in all cases. It can be seen that, firstly, in cases with a rotating

vessel, the maximum mixing quality is achieved after only about 20 s of mixing. The influence of the mixing tool speed is also relatively low in cases with a rotating vessel; a higher tool speed however tends to shorten the mixing time. The achievable final value for all cases with a rotating cylinder is $RSD < 0.05$, which is well above the value for statistical random mixing RSD_s. At higher tool speeds, the achievable mixing quality is slightly better than at lower speeds. The rotation of the vessel however has the strongest influence on the mixing homogeneity. This becomes clear when the curves without rotation of the vessel are compared. The drop in the *RSD* value is significantly slower, and the final value is also significantly higher than the final values for the tests with a rotating vessel. A slight improvement can be seen at higher tool speeds compared to slower speeds. These results suggest that the rotation of the vessel is essential for the homogenization of the mix. Table 3 shows the $RSD_{90\,\%}$ values,i.e.the mixing time after which 90 % of the steady-state final value is reached. This shows that the $RSD_{90\,\%}$ is reached faster without vessel rotation than with rotation. This indicates that the majority of the albeit poor mixing result is already achieved within a very short mixing time. The value is higher at higher tool speeds, which confirms that the mixing performance is slightly improved, but also takes longer to achieve. The $RSD_{90\,\%}$ values are reached significantly later when the vessel rotation is switched on, and there is also a slightly shorter mixing time $RSD_{90\,\%}$ found at higher tool speeds.

Table 3 also contains values for the mean squared displacement (MSD) as a function of mixing tool speed. It is calculated with the formula (8), where x,y and z stand for the position of a particle at different mixing times *t*. The MSD can be interpreted as the amount of spatial expansion of particles during mixing. The values are given as the mean ($\overline{MSD}$) and 95th percentile (MSD_{95}) since the ensemble average hides the underlying distribution character.

$$MSD(t) = \langle (x(t) - x(0))^2 \rangle + \langle (y(t) - y(0))^2 \rangle + \langle (z(t) - z(0))^2 \rangle \tag{8}$$

The simulated values for $\overline{MSD}$ and MSD_{95} shows the influence of the mixing tool speed on the spatial displacement of the particles during mixing. Hare (Hare et al., 2023) found in an experimental analysis of the MSD a value of around 0.001 m^2/s ($w_{tool} = 6$ m/s) in the same Eirich EL1.0 mixer type for a wet anode slurry process. Given that the particle mobility and MSD should generally increase in a dry system with negligible viscosity, the values found here seem plausible.

Table 3
Values for the RSD_{90}, $\overline{MSD}$ and MSD_{95} for different vessel and mixing tool speeds.

Parameter	40 m/s	5 m/s
$RSD_{90,0rpm}$	7.6 s	2.7 s
$RSD_{90,85rpm}$	16.8 s	17.5 s
$RSD_{90,170rpm}$	15.9 s	18.9 s
$\overline{MSD}$	0.040 m^2/s	0.030 m^2/s
MSD_{95}	0.070 m^2/s	0.050 m^2/s

4.4. Collision frequency, collision energy and shear rate

The DEM simulation model allows for the analysis of the particle collision frequency and energy during the mixing process. The collision frequency is calculated as the number of completed particle contacts per second and was evaluated for all contacts of particles with the mixing tool over a fixed time interval. Since the evaluation of every collision event is computationally expensive and must be performed on CPUs instead of faster GPUs, the evaluation took place after the flow field was fully established in the mixer and for time period of 1 s. As mentioned earlier the collision energy is no direct output parameter in the DEM software so that the collision energies are calculate via the formula (4) for all individual collision events and summed to give the total value per second. For many processes involving comminution the shear rates in a mixing system are used the describe its effect on particle breakage. Usually these processes involve higher viscous liquids since this facilitates the comminution process. The simulation of the Eirich mixer allows to calculate the shear rates in the mixer,

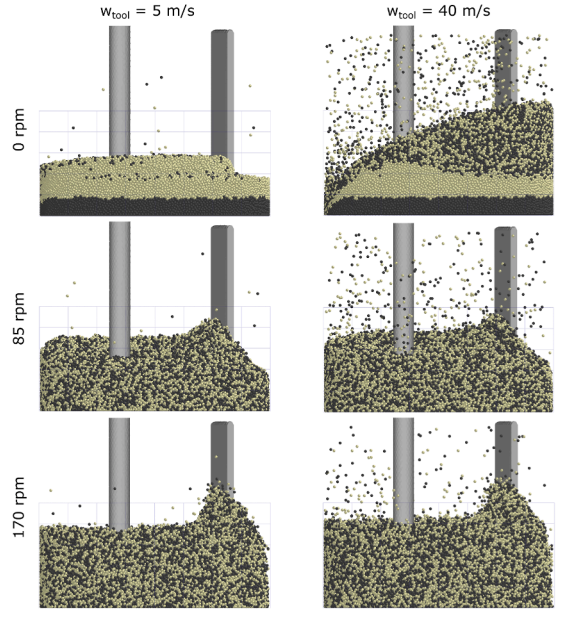

(a) Evaluation of the degree of mixing at a mixing time of 30s for two mixing tool speeds (5 m/s and 40 m/s) and three different vessel speeds (0 rpm, 85 rpm and 170 rpm); blue grid shows the used sample bins

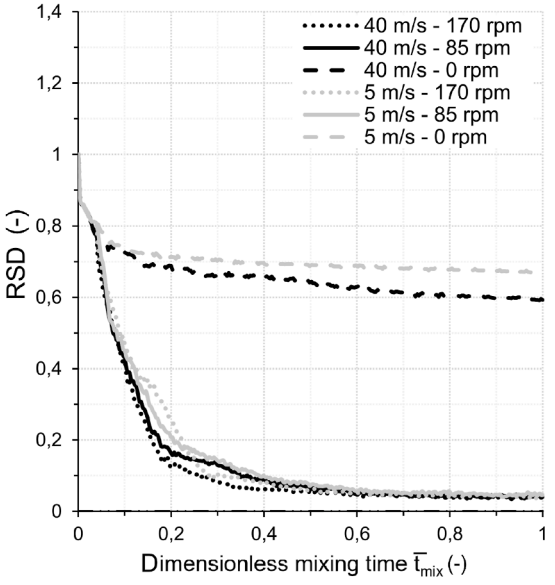

(b) Mixing degree RSD over dimensionless mixing time for different mixing tool and vessel speeds, the maximum simulation time is 30s

Fig. 7. Effect of mixing tool and vessel speed on the degree of mixing in Eirich EL1.0 mixer.

since this is a function of the established velocity field. The velocity field is interpolated from particle data in the mixer, after the flow is fully established. The method uses the in-software approach of a Gaussian weighting function of the particle data to continuum properties like the velocity field.

The magnitude of the shear rate can then further be calculated using the following formula:

$$|\dot{\gamma}| = \sqrt{2\frac{du^2}{dx} + 2\frac{dv^2}{dy} + 2\frac{dw^2}{dz} + \left(\frac{du}{dz} + \frac{dw}{dx}\right)^2 + \left(\frac{du}{dy} + \frac{dv}{dx}\right)^2 + \left(\frac{dw}{dy} + \frac{dv}{dz}\right)^2} \quad (9)$$

It contains the derivatives of the direction-dependent velocities u, v, w according to the x, y and z coordinates. The advantage of using this quantity is that the shear forces relevant for the comminution of carbon black in many processes are summarized in a single scalar quantity. Fig. 8(a) shows the calculated shear rate distributions $|\dot{\gamma}|$ for two different tool speeds of 5 m/s and 40 m/s, as well as two different vessel rotation speeds, 0 rpm and 170 rpm. The shear rates were evaluated in a horizontal section at a height corresponding to the maximum circumferential speed of the mixing tool. Although the maximum tool speed in the real mixer is limited to 30 m/s, we use a higher maximum tool speed for the simulations in order to evaluate even higher energy inputs. When looking at the calculated shear rate distribution in the mixer, the comparatively low shear rates of a maximum of 10 s^{-1} are noticeable. These values are one to two orders of magnitude lower compared to other types of mixers with comminution tasks, e.g. extruders, which can be attributed in particular to very small shear zones with usually under 1 mm in size. Although the circumferential speeds of the mixing tool in the EL1.0 are significantly higher than in a laboratory extruder, the material is not pressed through very narrow spaces that are located between the screw and housing or in between the screw elements.

The analysis of the shear rate distribution in the Eirich mixer also shows that the vessel speed has a significant influence on the shear in the particles. This shows an increase in the average shear rate by a factor of around 100, whereas the influence of the tool speed is comparatively low, which indicates a minor influence of the mixing tool on the overall shear in the mixture. The results of the shear rate analysis indicate that shear is not the dominant comminution mechanism during mixing in the Eirich high-intensity mixer. It is proposed that the comminution effect is primarily due to particle collisions with the rapidly rotating mixing tool. Fig. 8(b) shows the sum distributions of the relative collision velocities with the mixing tool at different circumferential speeds. The values show a clear increase in the average collision speed with increasing tool speed, which is synonymous with an increase in the kinetic energy of the particles after collision. A comparison of the sum curves of 5 m/s and 30 m/s tool speed shows a massive increase in particle velocities and corresponding kinetic energies, a circumstance that remained hidden in the analysis of the shear rate distribution, where hardly any increase in the mean shear rates with increasing tool speed was recognizable. The evaluations of operating modes and geometric changes to the mixer that follow in the next section will therefore be limited to a consideration of the collision rates and energies, as these are regarded as the main comminution mechanism in the Eirich mixer.

4.5. Effect of coarse graining size

The influence of the modeled particle size to represent the active material-carbon black mixture on the collision rates with the mixing tool was investigated. The cohesion number approach

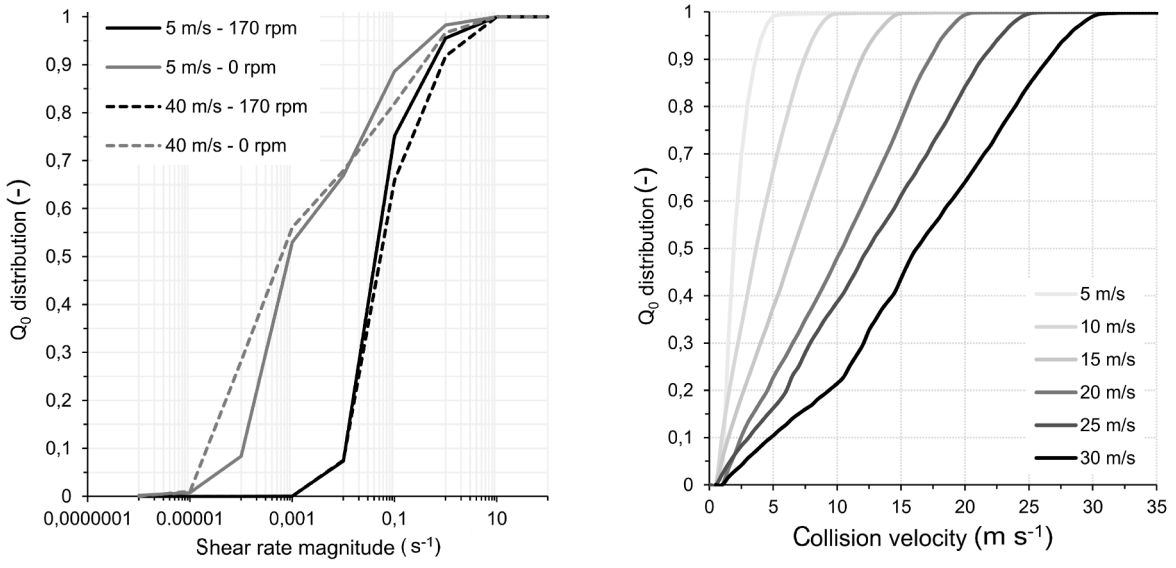

(a) Calculated shear rates at the mixing tool level for different mixing tool velocities and vessel rotation rates

(b) Calculated collision velocities between particles and mixing tool for different mixing tool velocities

Fig. 8. Comparison of calculated shear rates (a) and collision velocities (b) in Eirich EL1.0 mixer.

described above was used to take into account the surface-to-volume ratio changed by the particle diameter. To compare the original coarse-graining factor of CGF = 200, the particle sizes were reduced to 1.5 mm (CGF 150) and 1.0 mm (CGF 100) and the tool speeds of 5 m/s, 20 m/s and 40 m/s were investigated. The Coarse-Graining Factor was also increased to values of 400 ($d = 4$ mm) and 800 ($d = 8$ mm) to induce deviations from the base case. For better comparability the resulting collision rates were normalized to the total number of particles present in the system. Fig. 9(b) shows these normalized collision rates in comparison to the original model with a coarse-grain factor of 200. It can be seen that the normalized collision rates of CGF-150 and CGF-100 show a high level of agreement with the original system, which shows that a reduced calculation effort due to the increase in particle size leads to comparable results when assessing the collision frequency relevant to the comminution work. Increasing the Coarse-Grain-Factor to a value of 400 on the other hand shows deviations for the highest mixing tool speed of 40 m/s. For particle diameters of 8 mm (CGF-800) the deviations in the normalized collision rates are detectable for all mixing tool speeds. This indicates that the simulation model is not capable to produce comparable results for particle diameters bigger than 2 mm or a Coarse-Grain-Factor of 200.

Analyzing the resulting flow field in Fig. 9(a) shows very similar results for the overall appearance of material during mixing. The flow around the mixing tool and the wall scraper do not show any major differences, the resolution does however increase slightly with a lower Coarse Grain Factor. Fig. 9(b) reveals that with increasing mixing tool speeds the collisions rates decrease which is a common finding for all subsequent simulation results. This is attributed to a centrifuging effect of the mixing tool, which accelerates the material away from the mixing tool.

4.6. Effect of operation mode

All Eirich mixers can be operated in two basic modes. In co-current and counter-current operation. The experiments in this work were always carried out in co-current mode. However, the simulation model also allows a flexible and comparatively quick assessment of the effect of counter-current operation on the expected comminution work of the EL1.0 mixer. For this purpose, the collision rates for different tool speeds in counter-current operation were compared with those in co-current operation. The results can be found in Fig. 10(b). It is noticeable that the collision rates run almost parallel from a tool speed of 20 m/s. Up to 20 m/s, the collision rates for counter-current operation are in some cases significantly higher than those for co-current operation, which should generally lead to an improved comminution performance for these tool speeds. However, the increased energy input from 20 m/s leads to increased fluidization of the mixture, which in turn leads to reduced collision rates, so that no significant improvement in comminution performance can be expected at high tool speeds required for faster comminution.

Visual analyses of the resulting flow field (Fig. 10(a)) show that counter-current operation at a low tool speed of 5 m/s decreases the height of the material in the vessel which explains the increase in collision rates since more particles are present in the vicinity of the mixing tool. At higher tool speeds more material gets agitated and splashed into the vessel walls. This is very apparent when comparing the flow field at the maximum tool speed of 40 m/s to that of 5 m/s.

4.7. Effect of vessel inclination

The EL1.0 mixer from Eirich has the function of changing the angle of inclination of the mixing vessel. This can be used to enhance the particle flow e.g. in case of granulation. The angle was changed from 0° to a maximum of 30° in 10° increments. The influence of this change on the collision rates was investigated for the co-current operation mode. The result is shown in Fig. 11(b). It shows that the inclination of the mixing vessel is of less significance for the resulting collision rates. A slight increase can be registered with increasing vessel inclination, but this is of minor importance compared to other investigated modes of operation.

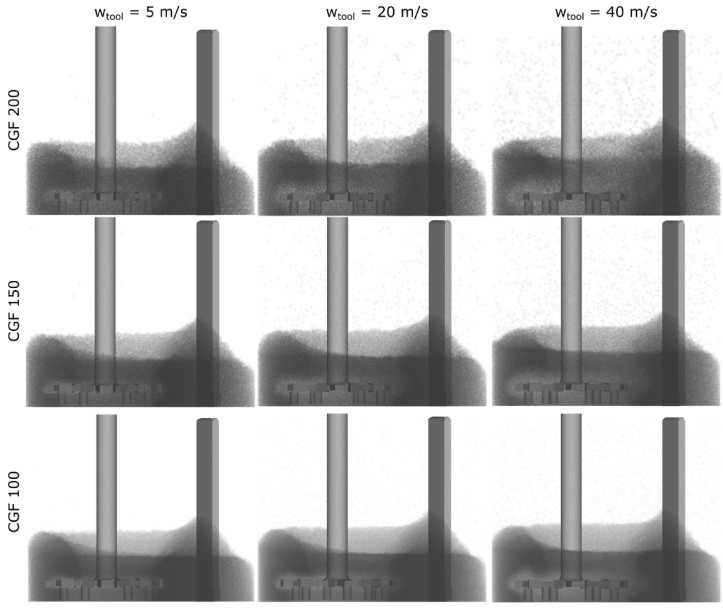

(a) Flow field for different mixing tool speeds and coarse grain factors (CGF) for a constant vessel speed of 85 rpm

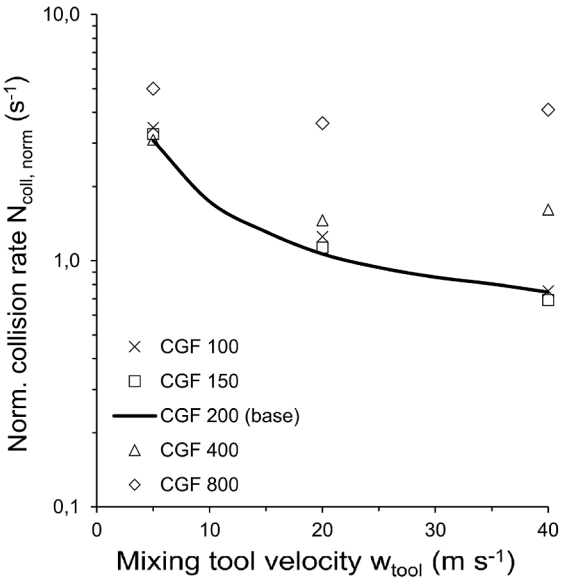

(b) Results for different coarse grain factors (CGF) on normalized collision rate

Fig. 9. Effect of particle size on the collision behavior and flow field in Eirich EL1.0 mixer.

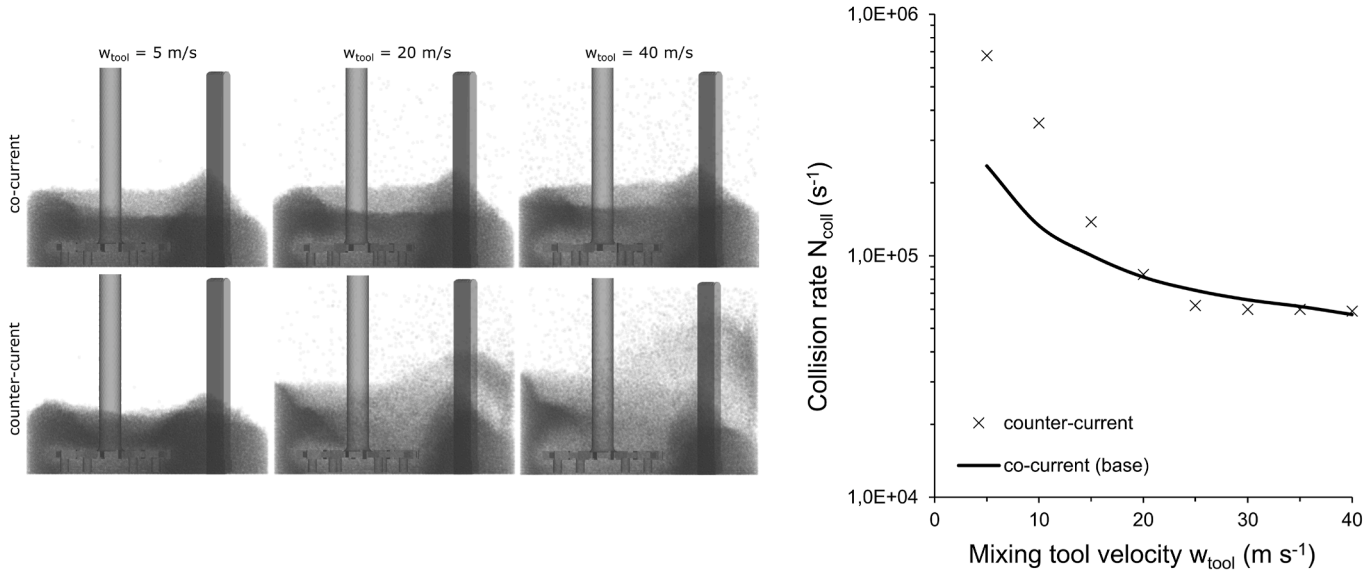

(a) Flow field in EL1.0 for co-current and counter-current operation mode at different mixing tool speeds

(b) Effect of operation mode on collision rates for different mixing tool speeds

Fig. 10. Effect of operation mode on the collision behavior and flow field in Eirich EL1.0 mixer.

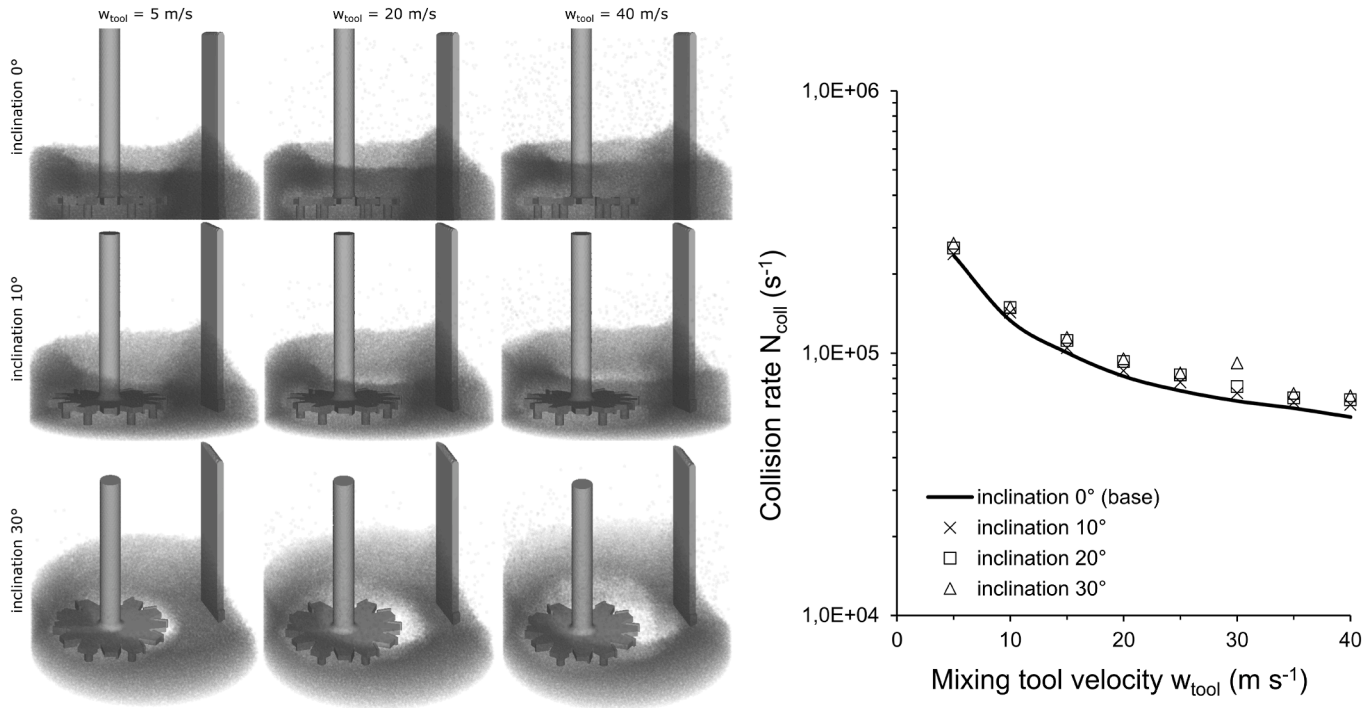

(a) Effect of vessel inclination of 0°, 10° and 30° on flow field in EL1.0 mixer

(b) Effect of vessel inclination of EL1.0 on collision rates for different mixing tool speeds

Fig. 11. Effect of vessel incination on the collision behavior and flow field in Eirich EL1.0 mixer.

The decreasing trend in the collision rate with increasing tool speed is also maintained when the vessel inclination is changed, which indicates that the centrifuging effect of the mixing tool cannot be compensated for by the changed material flow in the vessel.

4.8. Effect of vessel speed

The Eirich mixer has the option of operating the mixing vessel at two different rotational speeds. The influence of the vessel speed in co-current operation on the expected comminution performance in mixing operation was therefore investigated. In

addition to the standard operating mode with 85 rpm of the vessel (base), the second mode with 170 rpm and an operation without rotation of the mixing vessel (0 rpm) were investigated. The results are shown in Fig. 12(b). It can be seen that the collision rates at the maximum vessel speed are above the standard speed of 85 rpm for all simulated tool speeds. This may seem surprising at first, as a closer look at the flow field in the mixing vessel reveals a lower coverage of the mixing tool. The average amount of material in the area of the mixing tool is between 16 % and 35 % higher at a vessel speed of 85 rpm than at a vessel speed of 170 rpm. At the same time, however, the mass flow rate entering the stress area around the mixing tool increases by 56 % – 98 % with increasing vessel speed, which in turn leads to an increase in collision rates with the mixing tool. The higher collision rates for 170 rpm vessel speed may indicate that this operation mode is beneficial for the comminution task. This will be investigated further in a subsequent section, where the energy dissipation is analyzed.

At a vessel speed of 0 rpm the collision rates drop significantly below the rates for 85 rpm and 170 rpm. Comparing the tool speeds of 5 m/s for all cases reveal a significant expansion of the particle bed with higher vessel speeds. For 20 m/s and the higher the particle bed losses its near symmetrical form as particles accumulate at one vessel side. The analysis confirms that the vessel speed is not only important for mixture homogeneity, as shown earlier, but also for the collision rates with the mixing tool.

4.9. Effect of filling height

The EL1.0 mixer can be operated with a maximum filling volume of 1 L. Since a correlation between the filling volume and the collision rate with the mixing tool was suspected, two different filling levels, namely 1 L and 0.5 L, were compared with the filling level of the experimental tests (0.8 L). The result can be seen in Fig. 13(b). To ensure comparability with the different particle numbers, the collision rates were normalized with the total number of particles in the system. The solid line represents the normalized collision rate in the base case with a filling volume of 800 mL. It can be seen that the number of particle collisions with the mixing tool increases as the filling level increases. The normalized collision rate at a filling level of 1 L is above the collision rates of the reference filling level for all three investigated tool speeds of 5 m/s, 20 m/s and 40 m/s. At a lower fill level of 500 mL, however, these collision rates are below the reference. This shows that a lower fill level causes fewer particle collisions with the mixing tool, which is due to the fact that the material is centrifuged away from the tool. The higher the fill level in the mixer, the more resistance the particle bed offers to this centrifuging effect of the mixing tool, which results in a higher collision rate and ultimately also improves the expected comminution performance of the mixer.

Comparing the flow fields (Fig. 13(a)), a lower filling height results in more particles that are fluidized in the vessel which is more prominent with higher tool speeds. The agitation is damped however by particles above the mixing tool area for a higher filling volume.

4.10. Effect of mixing tool size

To investigate the potential optimization of the EL1.0 mixer, the influence of the mixing tool size on the collision rate was simulated. For this purpose, the size of the mixing tool was scaled to 125 % and 75 % of the original size.

The positioning of the tool was maintained in both cases, resulting in a smaller wall clearance in the case of the enlarged mixing tool and an increased wall distance in the case of the reduced mixing tool (see Fig. 14). The results of the collision rates are shown in Fig. 15(b). It can be seen that the size of the mixing tool has a significant influence on the collision frequencies with the particles. The collision rate increases with increasing diameter of the mixing tool, which on the one hand leads to an improved expected comminution performance, but also to an increased power requirement of the mixing tool. For the largest mixing tool,

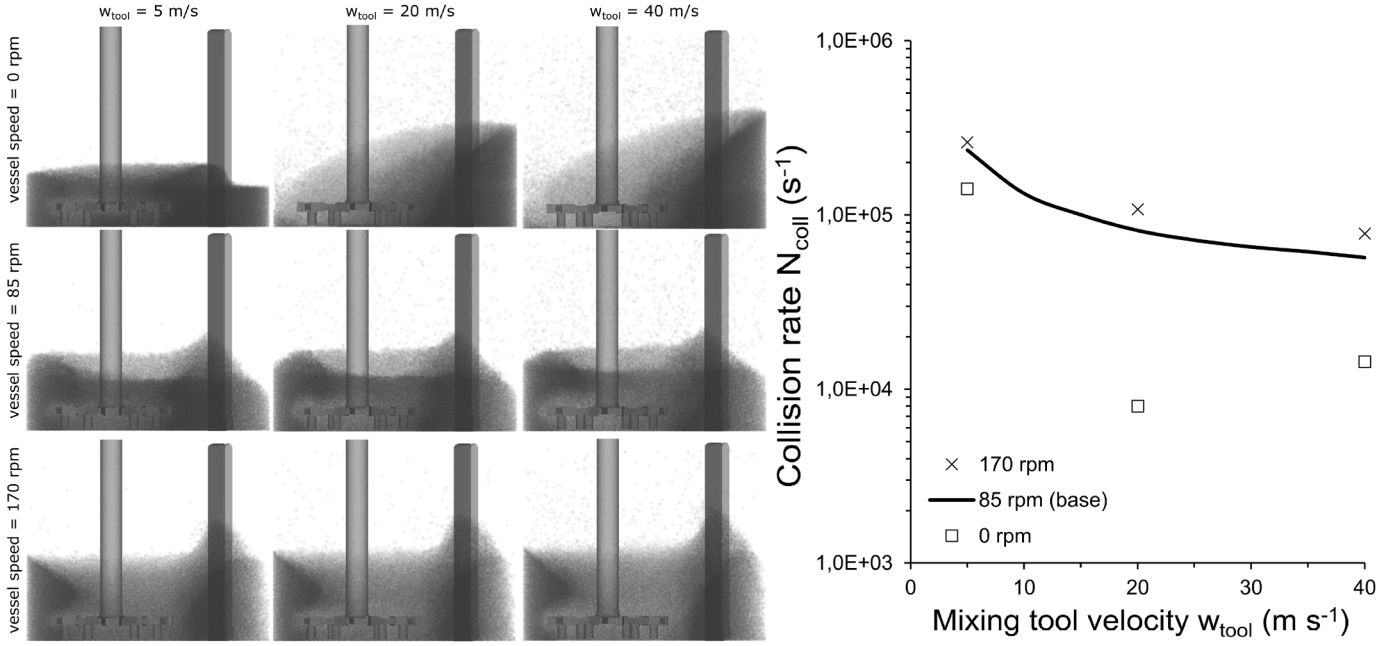

(a) Effect of vessel speed on the flow in the EL1.0 mixer

(b) Collision rates for the three possible vessel rotation speeds of 0 rpm, 85 rpm and 170 rpm

Fig. 12. Effect of vessel speed on the collision behavior and flow field in Eirich EL1.0 mixer.

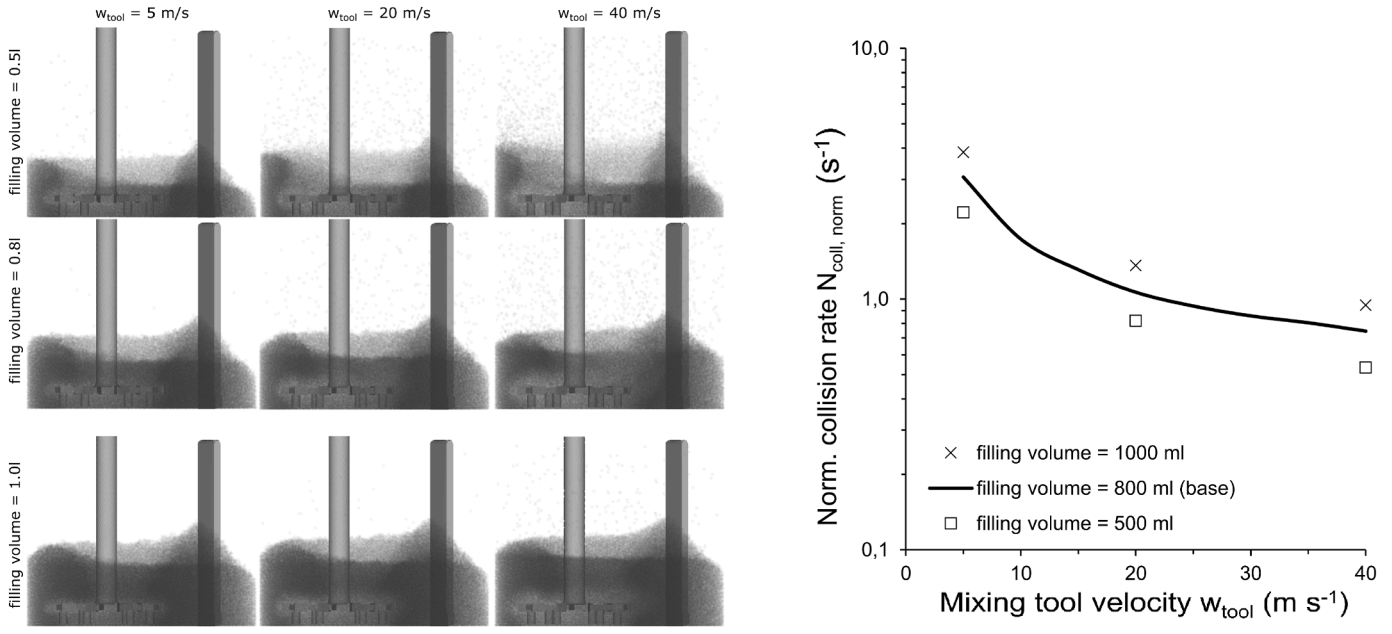

(a) Effect of the filling volume on the flow in the EL1.0 mixer

(b) Effect of filling volume in EL1.0 mixer on normalized collision rate for different mixing tool speeds

Fig. 13. Effect of filling volume on the collision behavior and flow field in Eirich EL1.0 mixer.

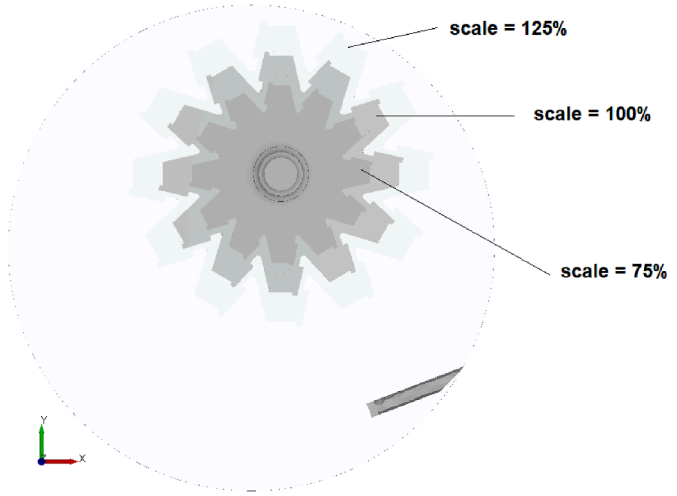

Fig. 14. Different mixing tool sizes used for simulations, scaled to 75 % and 125 % of the original size.

an almost constant collision rate was for tool speeds of 20 m/s and higher. This is in contrast to the trend of a decreasing collision rate for the original tool size and the reduced tool size, where not enough material can re-enter the collision zone once centrifugation becomes dominant. This result indicates that the overall performance may be optimized in future work by finding the best tool size to vessel ratio.

4.11. Effect of mixing tool pin number and blade addition

The mixing tool of the EL1.0 consists of 12 radially arranged teeth, as well as six vertically arranged pins as standard, which are oriented in the direction of the vessel base and have a distance between the vessel base and the tool of approximately 2 mm. To investigate the effect of the number of these pins, cases with 0, 4, 6 and 12 pins were calculated and evaluated. In addition, a new design for the mixing tool was created, which consists of additional blades arranged around the pins to facilitate the feeding of material into the area of the tool pins, aiming to reduce the centrifugation effect at higher tool speeds, that was unveiled by the simulation results. As the implementation of the blades results in an increase in diameter of the mixing tool, the rotation rates were reduced accordingly so that the same tool circumferential speeds are achieved with the new design. An overview of the modified geometries examined can be seen in Fig. 16.

The results in Fig. 17(b) show an improvement in the overall collision rates with the blade design of the mixing tool, which are above the base case for all tool speeds. The characteristic decrease in the collision rates for higher tool speeds, indicating centrifuging, is however still present with the blade design. Analysing the influence of the number of installed pins, there seems to be no significant increase in collision events when more than 6 pins are used. Slightly lower collision rates were detected when no pins are installed. When more than six pins are used the additional tool surface area does not introduce more material contacts, since not enough material is pushed into the mixing tool zone at the same time.

4.12. Energy specific collision and dissipation rate

Now that an analysis of various operating conditions and tool configurations has shown different absolute collision rates, a summary of the results will be given. For this purpose, the power-specific collision rate is calculated as the ratio of collision rate to tool power $n_{coll} = \frac{N_{coll}}{P_{tool}}$. The result is plotted for all investigated tool speeds in Fig. 18. The specific collision frequency allows an assessment of the extent to which the power introduced by the mixing tool can be converted into actual particle collisions. The decreasing curve of the specific collision rates with increasing tool speed again shows that a higher speed centrifuges the particles away from the tool and is therefore detrimental to the comminution performance of the mixer. It is noticeable that by looking at

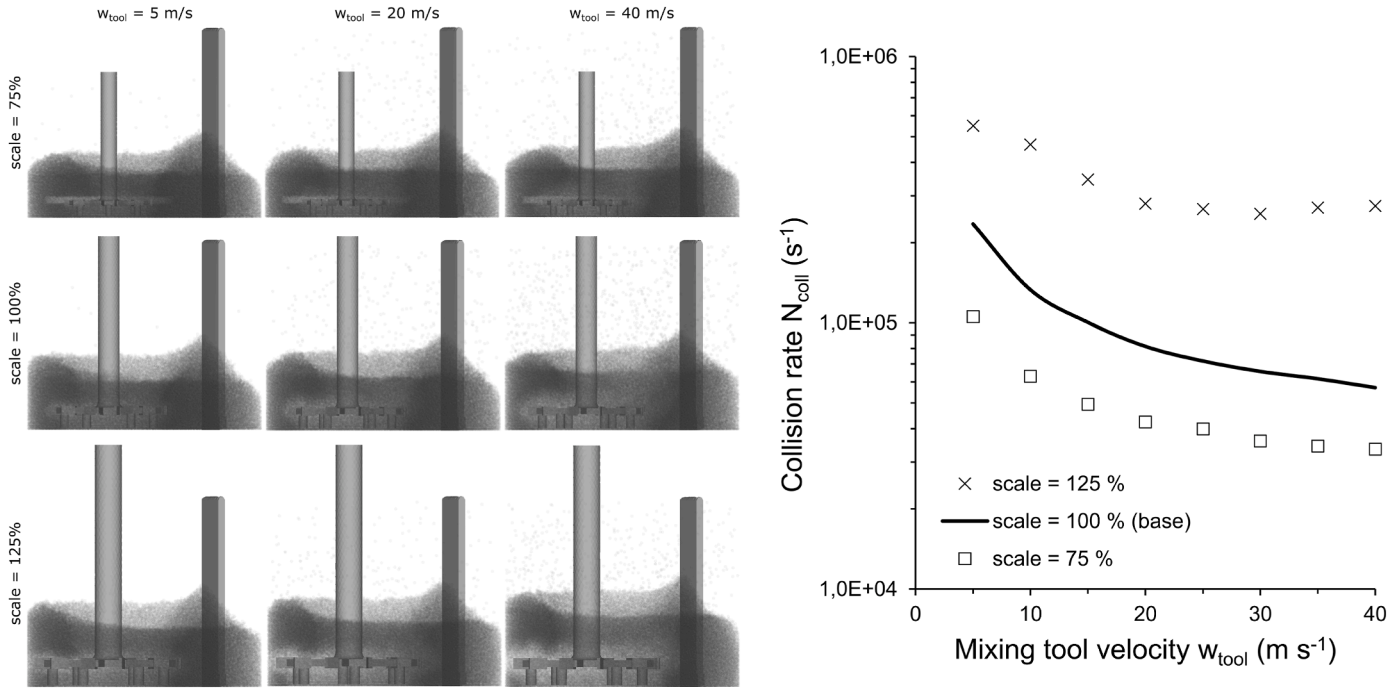

(a) Flow field results for three different mixing tool sizes

(b) Results for different mixing tool sizes on collision rate

Fig. 15. Influence of mixing tool size on the mixing performance in Eirich EL1.0 mixer.

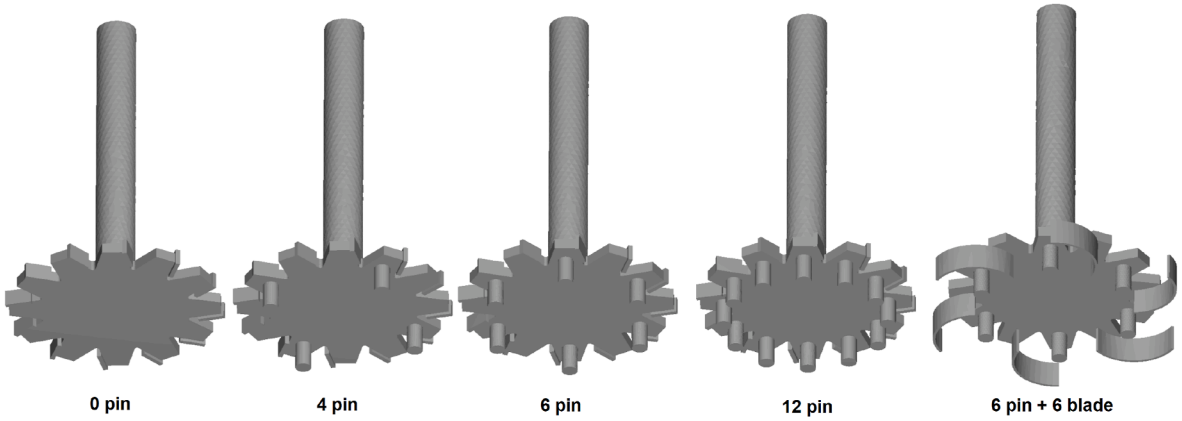

Fig. 16. Investigated mixing tools with different pin numbers (6 pins is the standard configuration).

the specific performance, all of the points examined, even if they lead to sometimes significantly different absolute collision rates as shown above, lead to quite similar results in the performance-specific analysis. Only the speeds of 5–15 m/s in the counter-current operating mode show a slight deviation to higher values. After that, hardly any significant differences can be observed up to a tool speed of 40 m/s. At the maximum tool speed investigated, an enlarged mixing tool appears to produce slightly better collision rates compared to the standard tool mode with a filling level of 500 mL. Also the blade design has comparable power specific collisions rates as the other investigated cases.

In order to assess not only the collision rates but also the collision energies, which is considered to be decisive for the comminution work, the mass specific total collision energy e_{coll} was investigated (Fig. 19(a)). It shows a clear trend to higher values for all simulated cases with increasing mixing tool speeds, which shows in general that the value of energy dissipation and therefor the expected amount of comminution is enhanced at higher tool speeds. There are however distinct differences in the amount of calculated collision energy between the different cases. For example a smaller tool scale leads to considerably lower collision energy compared to the blade design. Comparing all operating conditions in Fig. 19(a) points above the black line (base case) suggest an improvement in comminution performance. The calculated collision energy E_{coll} allows for a direct calculation of the mixing time needed to achieve a desired bulk density (compare Fig. 3(a)). For an exemplary final bulk density of 1400 kg/m^3, which indicated the best comminution degree in our previous work (Lischka et al., 2024), the average mixing time reduction for all mixing tool velocities compared to the base case in percent can be calculated. These conditions are in ascending order: a vessel speed of 170 rpm (20 % reduced mixing time), increased mixing

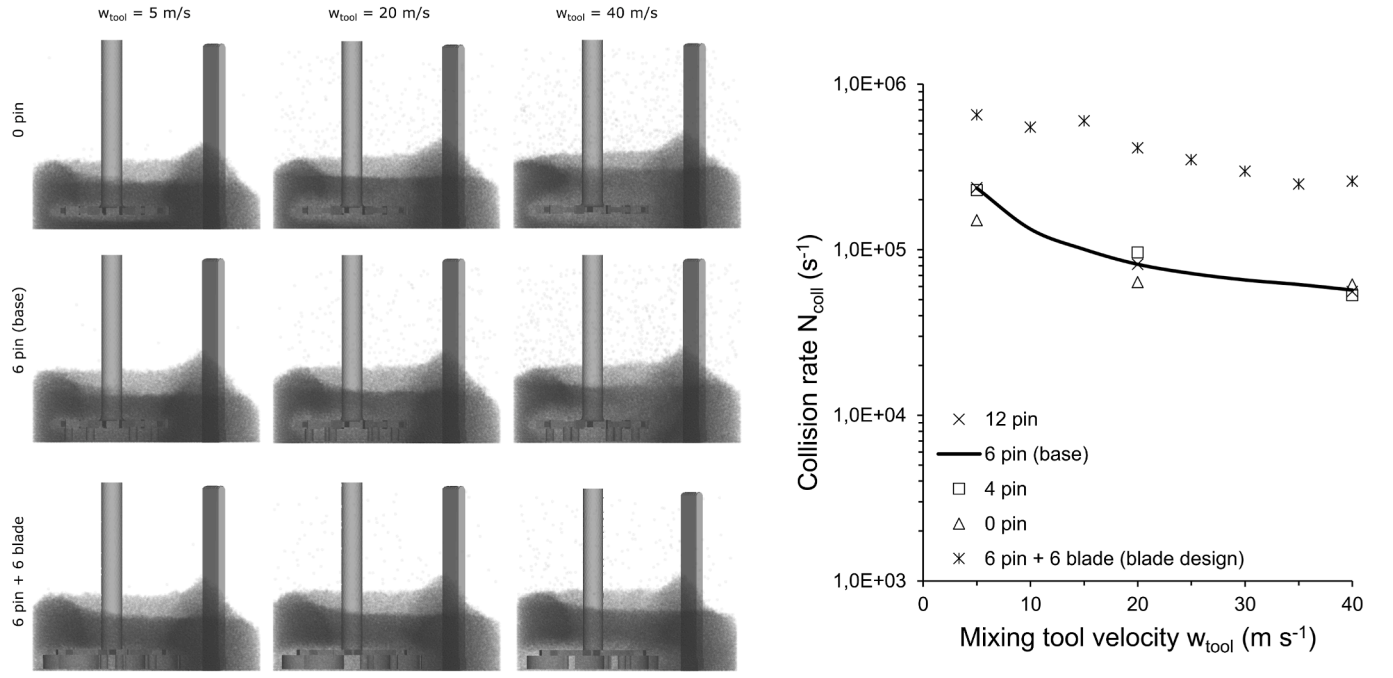

(a) Effect of mixing tool design (0 pin vs. 6 pin (base) and 6 pin + 6 blade) on the flow in the EL1.0 mixer

(b) Collision rates for the different mixing tool pin configurations (0 pin, 4 pin, 6 pin, 12 pin and 6 pin + 6 blade design)

Fig. 17. Effect of mixing tool design on the collision behavior and flow field in Eirich EL1.0 mixer.

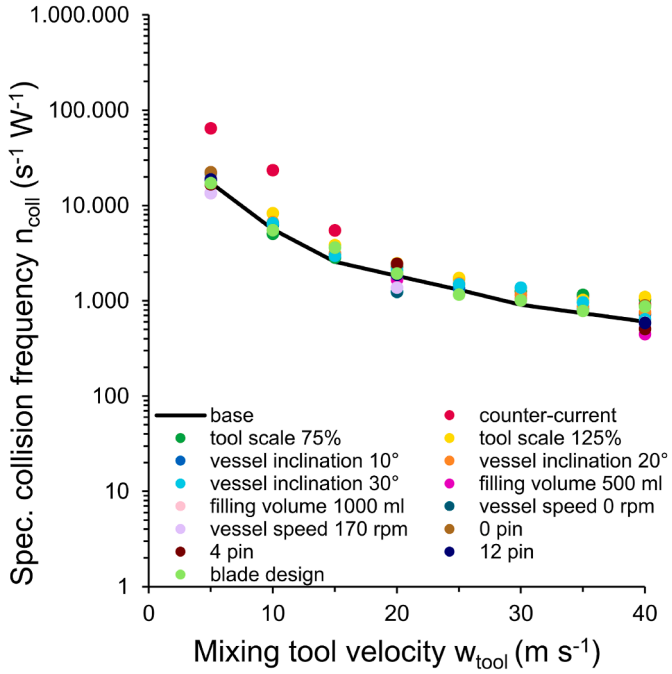

Fig. 18. Simulated power specific collision rates for all investigated mixing configurations and tool speeds.

tool size (56 % reduced mixing time) and the blade design mixing tool with a possible reduction of mixing time by up to 75 %.

In order the evaluate the cost for higher comminution rates, the power-specific collision energy rate is defined analogously to the specific collision rate as $\epsilon_{coll} = \frac{E_{coll}}{P_{tool}}$. This value indicates the maximum proportion of the collision energy available for the comminution work in relation to total power input. The results for all tool speeds investigated are shown in Fig. 19(b). On the one hand, the values around 10 % show that the majority of the collision energy for all tool speeds is not available for comminution work, but rather dissipated as heat due to friction or converted to kinetic energy. On the other hand, deviations are more pronounced for lower tool speeds, indicating that collision events are more sensitive to changes in the design or operational condition used at lower tool speeds. In general collision energy efficiency increases with higher tool speeds for most variations, showing that energy transfer is then dominated to a lesser extent by frictional losses. In total, the optimized design and operation parameters may reduce mixing time but are not more efficient then other variations, meaning better comminution performance comes at the cost of higher absolute power usage.

5. Conclusion

In this study, an experimental and simulative investigation of the mixing behavior in an Eirich EL1.0 intensive mixer during the dry mixing of Li-ion cathode material was carried out using the discrete element method. Experimental results have shown that the comminution of the conductive additive can be described independently of the selected mixer size by the specific energy supplied by the mixing tool into the mixed material via an increase in the powder bulk density, which was confirmed by measurements of the mean particle diameters using the Lumisizer sedimentation method.

The simulation model was calibrated with the aid of calibration experiments and then validated with good agreement using the power draw of the mixing tool for different circumferential speeds. It could also be shown that the impact stress of the mixed material with the rapidly rotating mixing tool can be regarded as the dominant comminution mechanism, as the shear rate distribution is less pronounced compared to other mixer types such as

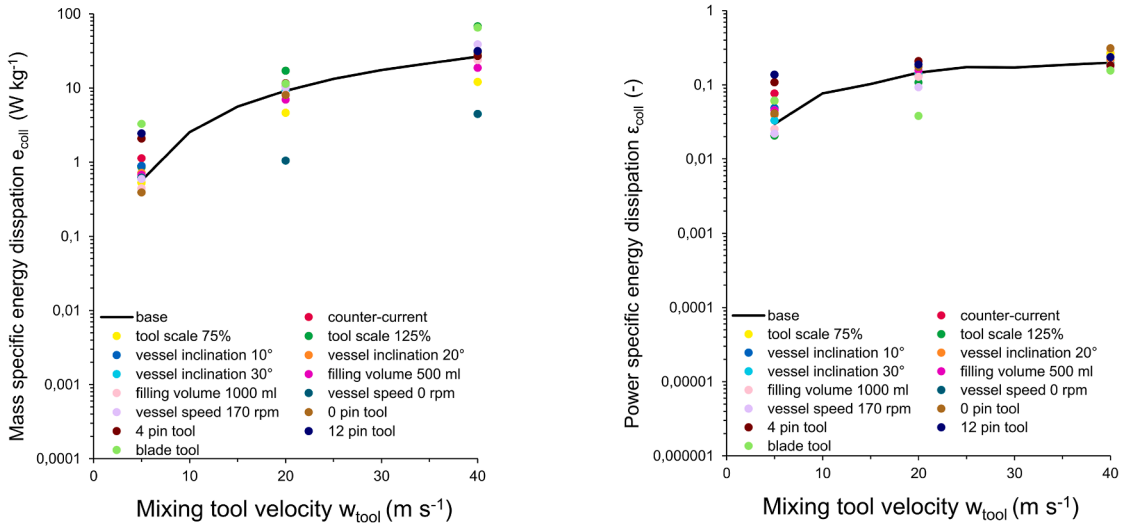

(a) Calculated values for energy dissipation for different mixing tool configurations and speeds

(b) Power specific energy dissipation over mixing tool speed for all simulation cases

Fig. 19. Comparison of the mass specific energy dissipation during collision (a) and power specific energy dissipation (b) in Eirich EL1.0 mixer.

extruders due to the design. Further investigation showed that mixture homogeneity is achieved on a macroscopic level within half a minute, nearly independent of the circumferential speed of the mixing tool. The rotation of the mixing vessel is essential for this. Whether the vessel is operated at 85 rpm or 170 rpm only plays a minor role. The collision rates of the particles with the mixing tool, the energy dissipation during the impact and the power input of the mixing tool were additionally used to assess the expected comminution of carbon black during mixing.

As the Eirich EL1.0 mixer can be operated in a wide variety of modes and parameters, these were examined with regard to an optimum. An improved collision frequency could be determined when operating in counter-current up to a tool speed of 20 m/s, but above 20 m/s to 40 m/s this is again at the level of co-current operation. In terms of improved energy input, counter-current operation is therefore not more advantageous than co-current operation. Inclining the vessel by 10°, 20° or 30° did not lead to any major deviation in collision frequency or energy dissipation compared to operation with an inclination of 0°. An increased vessel speed of 170 rpm resulted in a higher collision frequency compared to 85 rpm. The collision energy provided by the mixing tool is also elevated in case of higher vessel speed, which may reduce comminution time by up to 20 %. Significantly worse collision rates occur when the vessel rotation is switched off entirely, so this should be avoided. An increased filling level led to an increased collision frequency, which can be explained by a higher particle load in the area around the mixing tool. A higher filling level does however not translate to a higher collision energy transfer, indicating higher frictional losses. Accordingly, it may not be advantageous to carry out the comminution task with a maximum fill level. The investigation of the number of pins on the mixing tool showed that the mixing tool has almost constant collision rates regardless of the number of pins, whereby a number of 0 pins leads to poorer results, especially at low tool speeds. A design with six additional blades on the mixing tool showed enhanced collision rates. At the same circumferential speeds the absolute collision energies were also higher for the blade design compared to the reference, which shows the potential of optimizing the mixing tool design. In order to test the improved energy input during mixing, such a design can be tested virtually using the DEM simulation method presented here and then tested in practice by 3D printing the optimized mixing tool.

CRediT authorship contribution statement

Clemens Lischka: Writing – review & editing, Writing – original draft, Visualization, Validation, Methodology, Investigation, Formal analysis, Data curation, Conceptualization. **Hermann Nirschl:** Writing – review & editing, Supervision, Resources, Project administration, Funding acquisition.

Declaration of competing interest

The authors declare that they have no known competing financial interests or personal relationships that could have appeared to influence the work reported in this paper.

Acknowledgements

The authors gratefully thank the Federal Ministry of Education and Research for funding this work in the project Sim4Pro (grant number 03XP0242B) within the ProZell Cluster.

References

Al Alaween, W. H., Mahfouf, M., & Salman, A. D. (2017). Integrating the physics with data analytics for the hybrid modeling of the granulation process. *AIChE Journal, 63*(11), 4761–4773. https://doi.org/10.1002/aic.15831

Al hassn, A. Z., Jeßberger, S., Hounslow, M. J., & Salman, A. D. (2018). Multi-stage granulation: An approach to enhance final granule attributes. *Chemical Engineering Research and Design, 134*, 26–35. https://doi.org/10.1016/j.cherd.2018.03.038

Asylbekov, E., Mayer, J., Nirschl, H., & Kwade, A. (2023). Modeling of carbon black fragmentation during high-intensity dry mixing using the population balance equation and the discrete element method. *Energy Technology, 11*(5), Article 2200867. https://doi.org/10.1002/ente.202200867

Ax, K., Feise, H., Sochon, R., Hounslow, M., & Salman, A. (2008). Influence of liquid binder dispersion on agglomeration in an intensive mixer. *Powder Technology, 179*(3), 190–194. https://doi.org/10.1016/j.powtec.2007.06.010

Behjani, M. A., Rahmanian, N., Ghani, F.b. A. G., & Ali, H. (2017). An investigation on process of seeded granulation in a continuous drum granulator using DEM. *Advanced Powder Technology, 28*(10), 2456–2464. https://doi.org/10.1016/j.apt.2017.02.011

Bockholt, H., Haselrieder, W., & Kwade, A. (2013). Intensive dry and wet mixing influencing the structural and electrochemical properties of secondary

lithium-ion battery cathodes. *ECS Transactions, 50*(26), 25–35. https://doi.org/10.1149/05026.0025ecst

Burmeister, C., Titscher, L., Breitung-Faes, S., & Kwade, A. (2018). Dry grinding in planetary ball mills: Evaluation of a stressing model. *Advanced Powder Technology, 29*(1), 191–201. https://doi.org/10.1016/j.apt.2017.11.001

Daumann, B., Sun, X., Anlauf, H., Gerl, S., & Nirschl, H. (2010). Mixing agglomeration in a high-shear mixer with a stirred mixing vessel. *Chemical Engineering & Technology, 33*(2), 321–326. https://doi.org/10.1002/ceat.200900259

Frankenberg, F., Kissel, M., Burmeister, C. F., Lippke, M., Janek, J., & Kwade, A. (2024). Investigating the production of all-solid-state battery composite cathodes by numerical simulation of the stressing conditions in a high-intensity mixer. *Powder Technology, 435*, Article 119403. https://doi.org/10.1016/j.powtec.2024.119403

Gong, S., Zuo, Z., Xie, G., Lu, H., & Zhang, J. (2019). Numerical simulation of wet particle flows in an intensive mixer. *Powder Technology, 346*, 301–315. https://doi.org/10.1016/j.powtec.2019.02.004

Guan, X., Zhang, Z., Zhong, L., Wang, S., Xiao, M., Han, D., Huang, S., & Meng, Y. (2024). Novel Aliphatic polycarbonate binders for Solvent-free manufacturing High-loading cathodes of high-performance lithium-ion batteries. *Chemical Engineering Journal, 485*, Article 149983. https://doi.org/10.1016/j.cej.2024.149983

Hare, S. D., Werner, D., Windows-Yule, C. R. K., Kokalova Wheldon, T. Z., Kendrick, E., & Simmons, M. J. H. (2023). Use of positron emission particle tracking to assess mixing of a graphite-based lithium-ion anode slurry in an Eirich mixer. *Chemical Engineering Research and Design, 197*, 509–518. https://doi.org/10.1016/j.cherd.2023.08.007

Lischka, C., Gerl, S., Kappes, J., Chauhan, A., & Nirschl, H. (2024). Experimental simulative assessment of mixing quality for dry Li-Ion cathode production in an Eirich intensive mixer. *Powder Technology, 431*, Article 119072. https://doi.org/10.1016/j.powtec.2023.119072

Lischka, C., & Nirschl, H. (2023). Calibration of Li-ion cathode materials for discrete element method simulations. *Energy Technology, 11*(5), Article 2200849. https://doi.org/10.1002/ente.202200849

Mayer, J. K., Almar, L., Asylbekov, E., Haselrieder, W., Kwade, A., Weber, A., & Nirschl, H. (2020). Influence of the carbon black dispersing process on the microstructure and performance of Li-ion battery cathodes. *Energy Technology, 8*(2), Article 1900161. https://doi.org/10.1002/ente.201900161

Mayer, J. K., Bockholt, H., & Kwade, A. (2022). Inner carbon black porosity as characteristic parameter for the microstructure of lithium-ion electrodes and its effect on physical and electrochemical properties. *Journal of Power Sources, 529*, 231–259. https://doi.org/10.1016/j.jpowsour.2022.231259

Moreno-Juez, J., Tavares, L. M., Artoni, R., de Carvalho, R. M., Emerson, R.da C., & Cazacliu, B. (2021). Simulation of the attrition of recycled concrete aggregates during concrete mixing. *Materials, 14*(11). https://doi.org/10.3390/ma14113007

Muthancheri, I., Chaturbedi, A., Bétard, A., & Ramachandran, R. (2021). A compartment based population balance model for the prediction of steady and induction granule growth behavior in high shear wet granulation. *Advanced Powder Technology, 32*(6), 2085–2096. https://doi.org/10.1016/j.apt.2021.04.021

Niedziela, D., Schmidt, S., Steiner, K., Zausch, J., & Zemerli, C. (2015). Continuum numerical simulation of multiphase granular suspension flow in the context of applications for the mechanical processing industry. *International Journal of Mineral Processing, 136*, 50–55. https://doi.org/10.1016/j.minpro.2015.01.001

Rumpf, H. (1959). Beanspruchungstheorie der Prallzerkleinerung. *Chemie Ingenieur Technik, 31*(5), 323–337. https://doi.org/10.1002/cite.330310505

Schilde, C., Kampen, I., & Kwade, A. (2010). Dispersion kinetics of nano-sized particles for different dispersing machines. *Chemical Engineering Science, 65*(11), 3518–3527. https://doi.org/10.1016/j.ces.2010.02.043

Tokoro, C., Yamaoka, Y., Yuki, S., Shiozawa, T., & Owada, S. (2012). "Quantitative evaluation of the abrasion rate in attrition washing on lead contaminated soil from shooting ranges". English. *Materials Transactions, 53*(11), 1997–2003. https://doi.org/10.2320/matertrans.M2012240

Tokoro, C., Yamashita, T., Kubota, H., & Owada, S. (2009). Application of DEM simulation to an intensive mixer. *Resources Processing, 56*(3), 113–119. https://doi.org/10.4144/rpsj.56.113

Wenzel, V., Moeller, R. S., & Nirschl, H. (2014). Influence of mixing technology and the potential to modify the morphological properties of materials used in the manufacture of lithium-ion batteries. *Energy Technology, 2*(2), 176–182. https://doi.org/10.1002/ente.201300091

Zuo, Z., Gong, S., Xie, G., & Zhang, J. (2021). DEM simulation of binary mixing particles with different density in an intensive mixer. *Powder Technology, 383*, 454–470. https://doi.org/10.1016/j.powtec.2021.01.064

Zuo, Z., Wang, J., Gong, S., & Zhang, J. (2023). Effect of blade configuration on the mixing process of particles in an intensive mixer. *Particulate Science and Technology, 41*(8), 1088–1102. https://doi.org/10.1080/02726351.2023.2177216